COGNITIVE NEUROSCIENCE

What happens to your brain on the way to Mars

Vipan K. Parihar,[1] Barrett Allen,[1] Katherine K. Tran,[1] Trisha G. Macaraeg,[1] Esther M. Chu,[1] Stephanie F. Kwok,[1] Nicole N. Chmielewski,[1] Brianna M. Craver,[1] Janet E. Baulch,[1] Munjal M. Acharya,[1] Francis A. Cucinotta,[2] Charles L. Limoli[1]*

As NASA prepares for the first manned spaceflight to Mars, questions have surfaced concerning the potential for increased risks associated with exposure to the spectrum of highly energetic nuclei that comprise galactic cosmic rays. Animal models have revealed an unexpected sensitivity of mature neurons in the brain to charged particles found in space. Astronaut autonomy during long-term space travel is particularly critical as is the need to properly manage planned and unanticipated events, activities that could be compromised by accumulating particle traversals through the brain. Using mice subjected to space-relevant fluences of charged particles, we show significant cortical- and hippocampal-based performance decrements 6 weeks after acute exposure. Animals manifesting cognitive decrements exhibited marked and persistent radiation-induced reductions in dendritic complexity and spine density along medial prefrontal cortical neurons known to mediate neurotransmission specifically interrogated by our behavioral tasks. Significant increases in postsynaptic density protein 95 (PSD-95) revealed major radiation-induced alterations in synaptic integrity. Impaired behavioral performance of individual animals correlated significantly with reduced spine density and trended with increased synaptic puncta, thereby providing quantitative measures of risk for developing cognitive decrements. Our data indicate an unexpected and unique susceptibility of the central nervous system to space radiation exposure, and argue that the underlying radiation sensitivity of delicate neuronal structure may well predispose astronauts to unintended mission-critical performance decrements and/or longer-term neurocognitive sequelae.

INTRODUCTION

NASA has long been at the forefront of promoting manned exploration of space. As the duration of missions increases and extends beyond the protective magnetosphere of the Earth, astronauts will be exposed to a steady stream of low fluence but highly energetic and fully ionized nuclei that define the spectrum of galactic cosmic rays (GCRs) (1, 2). Charged particles within the GCR, referred to as HZE particles, derived from high (H) atomic number (Z) and energy (E), differ from terrestrial radiation types because the density of ionizing events deposited along the particles' trajectory leaves a track of damage through cells and tissues that prove difficult to resolve through cellular repair processes (3). The biologic impact of charged particles is exacerbated further by the secondary ionizations that extend from the primary particle track as delta rays, thereby extending considerably the range of resultant cellular damage throughout the various tissues of the body (4). Exposure to these energetic particles is inevitable because these particles traveling near the speed of light will traverse the hull of any spacecraft and tissue, and although strategies for increasing shielding (internally or via hull thickness) have been considered, they are offset by the practical limitations associated with the cost of sending increased payloads into space (5).

This dubious backdrop has led NASA and other space agencies to focus research studies on the understanding of charged particle radiation effects on biological systems with the goal of reducing uncertainties and estimating risks for developing various types of radiation-induced health disorders (3, 6). Although space radiobiology research has uncovered a wealth of potentially problematic health risks associated with charged particle exposure, none may prove more difficult to manage than those related to the functional decrements found in the brain that may occur during a space mission, endangering its success (7–10). Clinicians have known for decades that patients subjected to cranial radiotherapy for the control of brain malignancies develop severe and progressive cognitive deficits that never resolve (11, 12). Although clinical doses and radiation types differ substantially from those found in space, more recent research investigating the effects of space-relevant fluences of charged particles has uncovered convincing evidence that, at these low exposure levels, cognitive deficits occur and persist (9, 10). Even though the underlying mechanisms are certain to be multifaceted, recent evidence has now revealed the capability of radiation to significantly compromise the structural complexity and synaptic integrity of neurons throughout different regions of the brain (13–15). Although similar types of changes have been shown to underly a host of neurodegenerative conditions that exhibit dementia (16–21), it remained uncertain how ionizing radiation exposure affected more mature neuronal subtypes to compromise neurotransmission. Here, we show that very low doses of charged particles can compromise cognitive performance over extended times through mechanisms involving the reduction of dendritic complexity and alterations in synaptic integrity.

RESULTS

Cognitive testing

To assess the functional consequences of charged particle exposure on the brain, we performed behavioral tests on mice 6 weeks after being exposed to ^{16}O or ^{48}Ti particles using novel object recognition (NOR) and object in place (OiP) tasks. These tasks interrogate the functional connectivity of the medial prefrontal cortex (mPFC) and hippocampus

[1]Department of Radiation Oncology, University of California, Irvine, Irvine, CA 92697–2695, USA. [2]Department of Health Physics and Diagnostic Sciences, University of Nevada, Las Vegas, Las Vegas, NV 89154, USA.
*Corresponding author. E-mail: climoli@uci.edu

and depend on the ability to discriminate novelty from previous situations involving either similar or dissimilar objects placed at familiar or novel locations (22, 23). Compared to controls, animals exposed to low-dose ^{16}O or ^{48}Ti HZE particles exhibited significant behavioral decrements on both NOR (Fig. 1A) and OiP (Fig. 1B) tasks. Although only the higher 30 cGy dose of ^{16}O particles caused significant deficits on either task, both 5 and 30 cGy doses of ^{48}Ti particles led to marked and

significant reductions in the discrimination index (DI) for each task. Reduced DI values were on average ninefold lower after exposure to ^{48}Ti particles and were not dose-dependent. The persistent reduction in the ability of irradiated animals to react to novelty after such low-dose exposures suggests that space-relevant fluences of HZE particles can elicit long-term cognitive decrements in learning and memory.

Dendritic complexity of irradiated mPFC neurons

To assess the potential causes of charged particle–induced cognitive dysfunction, we conducted morphometric analyses on neurons within the prelimbic layer of the mPFC after cognitive testing. The presence of brightly fluorescent neurons within the Thy1-EGFP (enhanced green fluorescent protein) transgenic strain greatly facilitates the structural analyses of select neurons throughout the brain (14, 15). Confocal-derived digital reconstructions reveal extensive arborization of mPFC neurons (Fig. 2, 0 cGy), and exposure to charged particles (Fig. 2, 30 cGy) showed subsequent reductions in dendritic complexity (green) and spine density (red). Quantification of structural parameters revealed marked and significant reductions in the number of dendritic branches, branch points, and overall dendritic length after nearly every dosing paradigm used (Fig. 2). Although most of these changes were not found to be dose-responsive, data indicate clearly that space-relevant fluences of charged particles can elicit significant and persistent reductions in the structure of mPFC neurons.

Spine density in irradiated mPFC neurons

Higher-resolution analysis of reconstructed dendritic segments also revealed marked effects of charged particle exposure on spine density. Charged particle irradiation using either ^{16}O or ^{48}Ti particles at 5 or 30 cGy elicited significant and persistent reductions in the total number of dendritic spines when quantified 8 weeks after exposure (Fig. 3). When these dose-independent changes were normalized to dendritic length (that is, 10 μM), low fluences of charged particles were found to elicit marked reductions in dendritic spine density after each irradiation paradigm (Fig. 3).
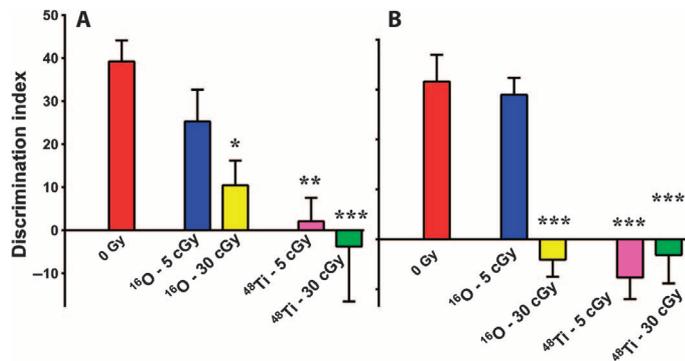

Fig. 1. Behavioral deficits measured 6 weeks after charged particle exposure. (A) Performance on a NOR task reveals significant decrements in recognition memory indicated by the reduced discrimination of novelty. (B) Performance on an OiP task shows significant decrements in spatial memory retention, again indicated by a markedly reduced preference to explore novelty. *$P = 0.05$, **$P = 0.01$, ***$P = 0.001$, analysis of variance (ANOVA).

Correlating altered cognition to spine density

To determine the functional impact of certain morphometric changes in the brain, we correlated the DI of individual mice to their respective spine densities (1.3 mm^2) after each irradiation paradigm. Plotting dendritic spine density against the corresponding performance of animals subjected to the OiP task revealed interesting and significant trends (Fig. 4). Compared to controls, all irradiated cohorts exhibit trends toward reduced dendritic complexity and lower DI values. Whereas some of these trends did not reach significance (for example, ^{16}O exposure; Fig. 4A), exposure to 30 cGy of ^{48}Ti particles correlated
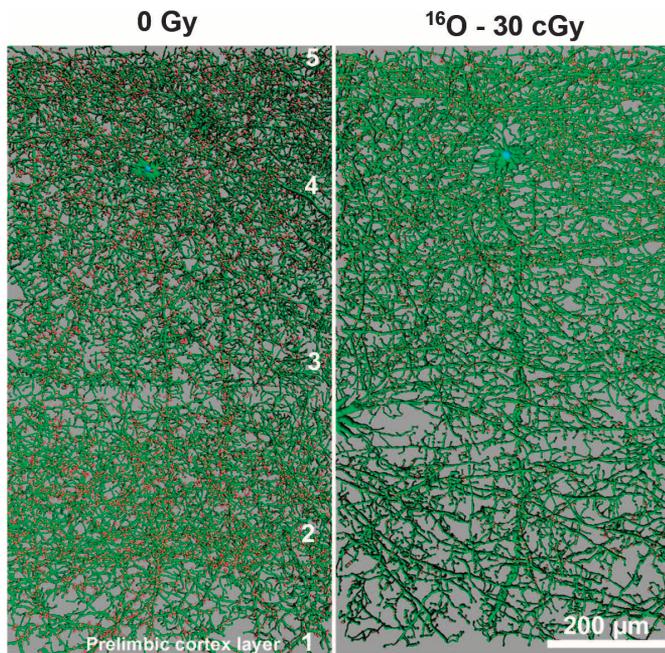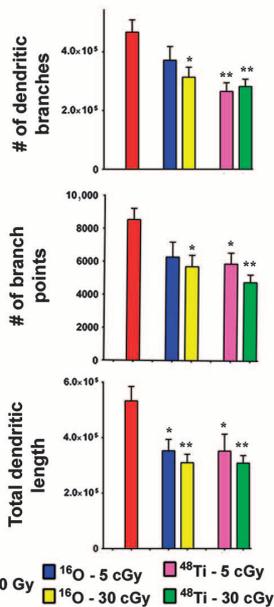

Fig. 2. Reduced dendritic complexity of neurons in the prelimbic layer of the mPFC 8 weeks after HZE particle irradiation. Digitally reconstructed images of EGFP-positive mPFC neurons before (0 cGy) and after (30 cGy) irradiation showing dendrites (green) and spines (red). Quantification of dendritic parameters (bar charts) shows that dendritic branching and length are significantly reduced after low-dose (5 and 30 cGy) exposure to oxygen (^{16}O) or titanium (^{48}Ti) particles. *$P = 0.05$, **$P = 0.01$, ANOVA.

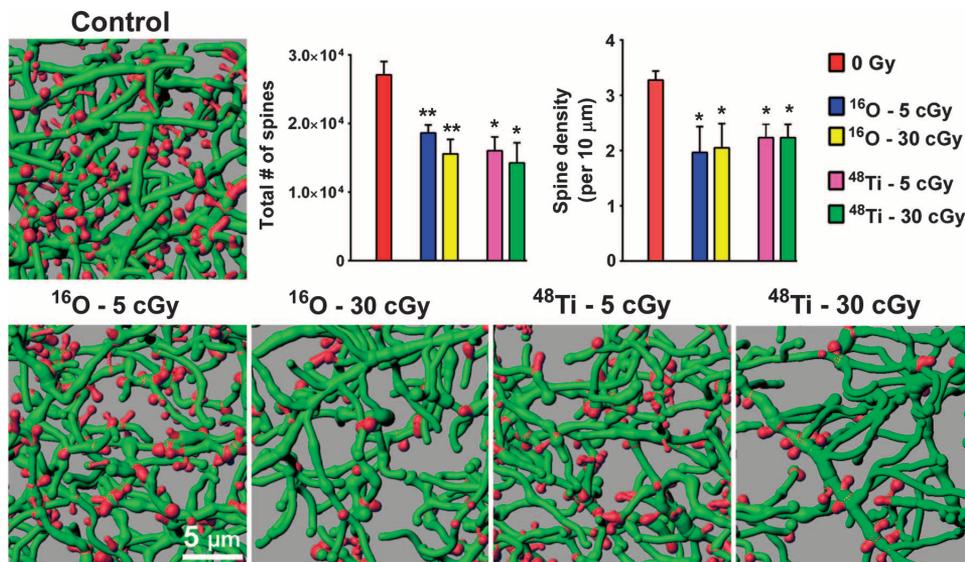Parihar et al. Sci. Adv. 2015;1:e1400256   1 May 2015

2 of 6

Fig. 3. Reductions in dendritic spine density in the mPFC after HZE particle exposure. Representative digital images of 3D reconstructed dendritic segments (green) containing spines (red) in unirradiated (top left panel) and irradiated (bottom panels) brains. Dendritic spine number (left bar chart) and density (right bar chart) are quantified in charged particle–exposed animals 8 weeks after exposure. *$P = 0.05$, **$P = 0.01$, ANOVA.
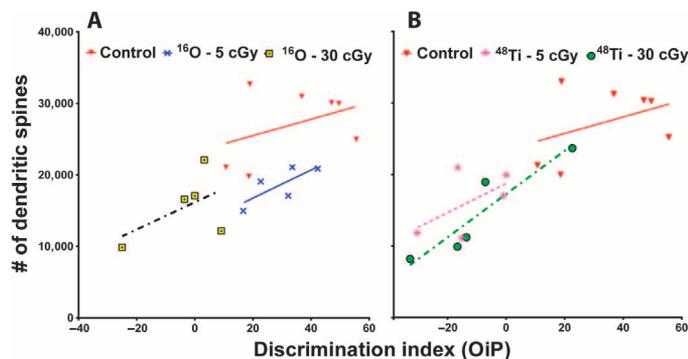

Fig. 4. Correlation of spine density with DI. Dendritic spine density (per 1.3 mm^2) is plotted against the corresponding performance of each animal on the OiP task. (**A** and **B**) Reduction in spine number after irradiation is correlated with reduced DI for novelty after exposure to 5 or 30 cGy of ^{16}O (A) or ^{48}Ti (B) charged particles. The correlation between spine density and DI is significant for the 30 cGy ^{48}Ti data (green circles; $P = 0.016$).

significantly with reduced DI (Fig. 4B, green circles). These data demonstrate the benefits of correlating radiation-induced changes in neuronal morphometry to behavioral performance and demonstrate that certain structural changes in neurons correspond to select deficits in cognition.

PSD-95 synaptic puncta after irradiation of mPFC neurons

To complement structural analyses, we quantified the levels of synaptic puncta from deconvoluted confocal images of tissue sections subjected to immunohistochemical staining for postsynaptic density protein 95 (PSD-95) (Fig. 5). High-resolution imaging of control and irradiated brain tissue revealed a consistent, albeit dose-independent, increase in the yield of PSD-95 puncta after HZE particle irradiation.

Exposure to either dose of ^{16}O or ^{48}Ti particles increased PSD-95 levels by ~60% along neurons in the mPFC. These data indicate that, in addition to structural changes, charged particle exposure elicits persistent and significant alterations in the prevalence of certain synaptic proteins. These changes, however, did not reach statistical significance when individual behavioral performance was plotted against synaptic puncta (fig. S1).

DISCUSSION

Past work by others and us has shown that relatively low doses of charged particles can elicit various cognitive decrements in the brain ranging from defects in executive function to spatial learning and memory (8–10). For astronauts, the need to optimize their performance in response to unanticipated situations (that is, executive function) will be critical and will depend on the operation of more basic cognitive processes. Cognitive tasks that interrogate specific regions of the brain have identified wide-ranging radiation-induced deficits mapping to both defined and more global regions that include the frontal and temporal lobes containing the mPFC and hippocampus, respectively (8–10, 13). The behavioral tasks selected for this study measure episodic memory retention (NOR), which depends on intact mPFC and hippocampal function, and spatial memory retention (OiP), which also depends on intact hippocampal function in addition to contributions from the prefrontal and perirhinal cortices. The present data now clearly demonstrate the importance of the mPFC because low-dose charged particle irradiation disrupts mPFC function, leading to deficits in NOR and OiP behavioral performance (Fig. 1). Neurons within the mPFC relay information between cortical, hippocampal, and other brain regions (24–26), and cognitive deficits affecting NOR and/or OiP performance indicate that neurotransmission within these circuits has been perturbed.

At these low doses and high particle velocities, neurons (as well as other cell types) will incur direct particle traversals, whereas energetic electrons produced by ionizations along the particle track will extend radially out to about 1 cm with the density of these electrons $(22/8)^2$ ~7.6 times higher for ^{48}Ti compared to ^{16}O. For the particles and doses used in this study, one can compare the fluences per square micron relative to the size of several neuron structures including the soma (~100 μm^2), dendritic tree (>1000 μm^2), and filopodia (~5 μm^2), as well as other spine types. The probability of direct particle traversals of these structures varies with the linear energy transfer and dose. For doses of 5 to 30 cGy, the mean numbers of direct traversals are as follows: soma, 0.25 to 1.5 for ^{48}Ti and 1.9 to 11.3 for ^{16}O; dendritic tree, 2.5 to 15 for ^{48}Ti and 19 to 114 for ^{16}O; and filopodia, 0.013 to 0.075 for ^{48}Ti and 0.1 to 0.57 for ^{16}O. Therefore, although most cell nuclei/soma will be directly traversed at these low fluences, direct traversals to spines are rare events. Furthermore, direct and indirect
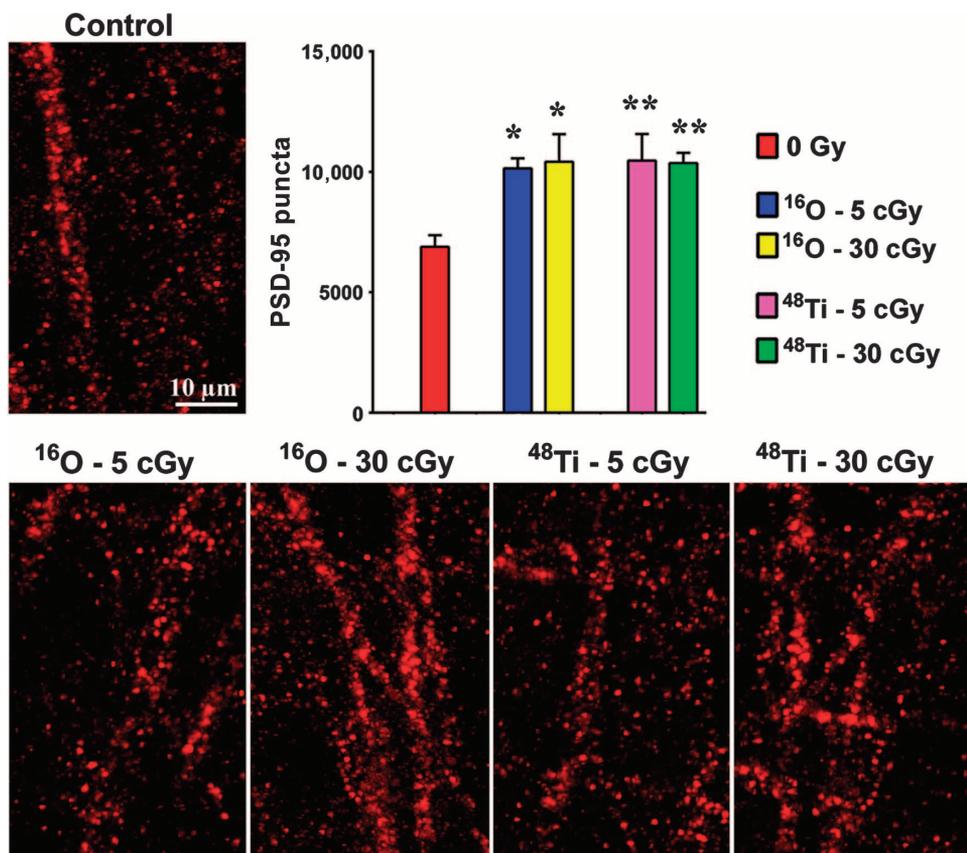
Fig. 5. Changes in PSD-95 synaptic puncta in the mPFC 6 weeks after exposure to 5 or 30 cGy of ^{16}**O or** ^{48}**Ti charged particles.** Fluorescence micrographs show that irradiation leads to increased expression of PSD-95 puncta (bottom) in mPFC neurons after irradiation compared to controls (top left). Quantified PSD-95 puncta (bar chart) in the mPFC. *$P = 0.05$, **$P = 0.01$, ANOVA.

play a pivotal role in organizing and recruiting proteins and receptors in the synaptic cleft (27–29). Thus, alterations to the structure of neurons and the stoichiometry of synaptic proteins likely play a contributory if not causal role in disrupting neurotransmission after charged particle exposure, manifesting as behavioral decrements on tasks dependent on intact circuitry in the mPFC. These cognitive deficits could prove hazardous during the course of a Mars mission.

To further establish the functional relevance of current findings, we correlated radiation-induced changes in dendritic spines and synaptic puncta with individual behavior performance on the OiP task. Exposure to 5 or 30 cGy of either ^{16}O or ^{48}Ti particles led to significant reductions in mPFC dendritic spines compared to unirradiated controls and, when plotted against DI on the OiP task, showed consistent trends between reduced dendritic spine density and lower DI values (Fig. 4). Significant correlations were found at the 30-cGy dose, where data indicate that behavior on the OiP task was impaired (DI $\cong$ −20) when spine densities dropped below $20,000/0.026\ mm^3$ in the mPFC. As the structural correlates of learning and memory, dendritic spines are critical to cognitive function (29, 30), and it stands to reason that optimal performance of rodents or humans engaged in complicated tasks will be compromised once spine numbers are reduced below certain threshold levels. Similarly, optimal cognitive performance depends on synaptic integrity, and increased levels of PSD-95 known to disrupt the balance between excitatory and inhibitory neurotransmission (31, 32) were clearly evident after exposure to HZE particles (Fig. 5). Although not significant, data revealed that as the number of PSD-95 puncta increased above $8000/0.0018\ \mu m^3$ in the mPFC, exploration of novelty trended downward (DI $\leq$ −20) on the OiP task (fig. S1). Thus, low-dose exposure to HZE particles elicits persistent cognitive deficits that correlate significantly with specific morphometric changes to neurons (spine density) that fall within certain threshold levels.

Assigning predictive value to structural and synaptic parameters relevant to cognitive performance after radiation exposure remains a significant challenge (33), inasmuch as defining the criteria for critical thresholds is confounded by inherent limitations extrapolating behavioral data from rodents to humans. Our data clearly demonstrate that low-dose HZE particle exposure leads to persistent impairments in behavioral performance as manifested by the inability to discriminate novelty of object or location. Although we cannot simulate exactly the complex and prolonged charged particle irradiation pattern encountered in space, the present data do demonstrate that there is some likelihood of developing certain radiation-induced cognitive deficits. Deep space travel is dynamic and involves many unique situations

(delta ray) hits with nonnuclear (dendritic and axonal) structures increase the cross section for charged particle interactions with cells (1). This may, in part, explain the relative lack of dose response, where very small dose thresholds may manifest as all-or-nothing responses to sparse particle traversals through the brain. Therefore, if a single particle traversal has the potential to ionize targets within a 1-cm cylindrical radius through the brain, then the probability of any given neuronal structure incurring multiple ionizations during a mission to Mars approaches unity (3). Thus, very low fluences of charged particles can interact with a considerable number of neural cell types and circuits, and data clearly indicate that significant deficits in learning and recall memory persist long after exposure.

To establish cause and effect, we analyzed mice subjected to cognitive testing to determine whether certain neurons within the region known to be interrogated by these tasks (that is, the mPFC) contained measurable alterations to their structural and/or synaptic integrity. Reductions in dendritic complexity and spine density observed in this study after exposure to space-relevant fluences of charged particles corroborate past findings with γ-rays (14) and protons (15), less densely ionizing radiations found both on Earth and in space. These data are the first evidence that low doses of charged particles elicit marked and persistent changes in neuronal structure in the mPFC. These detrimental effects coincided with increases in PSD-95 protein, known to

and environments that complicate decisions for defining acceptable risks for developing HZE particle–induced neurocognitive decrements during and/or after spaceflight. Although the impairment of neurocognitive performance is undesirable in any circumstance, the impact of such decrements on the success of a deep space mission is likely to be especially problematic because of delayed communication that results in an increased necessity for astronaut autonomy and the ability to make critical decisions quickly. Therefore, resolution of these health risk uncertainties associated with the unavoidable exposure to charged particles in the GCR represents an increasing priority for NASA as they plan for longer-duration missions into this unique environment. The exquisite susceptibility of neuronal architecture to the effects of charged particles reported here has important implications for human exploration into space and defines the need to further our understanding of radiation effects in the central nervous system as NASA prepares astronauts for one of the greatest adventures of humankind.

MATERIALS AND METHODS

Additional experimental procedures can be found in the Supplementary Materials.

Animals, heavy ion irradiation, and tissue harvesting

All animal procedures were carried out in accordance with National Institutes of Health and Institutional Animal Care and Use Committee guidelines. Six-month-old male transgenic mice [strain Tg(Thy1-EGFP) MJrsJ, stock no. 007788, The Jackson Laboratory] harboring the Thy1-EGFP transgene were used in this study. Mice were bred and genotyped to confirm the presence of Thy1-EGFP transgene. Charged particles (^{16}O and ^{48}Ti) at 600 MeV/amu were generated and delivered at the NASA Space Radiation Laboratory (NSRL) at Brookhaven National Laboratory at dose rates between 0.5 and 1.0 Gy/min. Dosimetry was performed, and spatial beam uniformity was confirmed by the NSRL physics staff.

Behavioral testing

Six weeks after irradiation, mice were subjected to NOR and OiP tasks to quantify behavioral performance. NOR and OiP rely on intact hippocampal and prefrontal cortex function. Whereas NOR is a measure of preference for novelty, OiP is a test of associative recognition memory, which depends on interactions between the hippocampus, perirhinal, and medial prefrontal cortices. Behavior was conducted as described previously (13). The following expression was used to calculate the DI:

$$\left[\left(\frac{\text{Time spent exploring novel object}}{\text{Total exploration time}}\right) - \left(\frac{\text{Time spent exploring familiar object}}{\text{Total exploration time}}\right)\right] \times 100$$

Confocal microscopy, imaging, and neuronal morphometry

The expression of EGFP in specific subsets of neurons provides detailed visualization and quantification of neuronal architecture. In previous studies, we demonstrated that γ-irradiation or proton irradiation reduced dendritic complexity of hippocampal granule cell neurons. Here, we focused on neurons in the prelimbic layers of the mPFC using rigorously defined morphometric criteria. Parameters of neuronal structure that were identified and quantified through image reconstruction and deconvolution using the IMARIS software suite (Bitplane

Inc.) included the cell body, dendritic and axonal length, branching and branch points, dendritic complexity, spines, and boutons.

For dendritic analysis, paraformaldehyde-fixed 100-μm-thick mPFC sections were prepared to image neurons within the prelimbic area (in reference to bregma, 2.80 to 1.50 mm) using confocal microscopy. In each cohort ($n = 5$), three sections per animal were scanned to generate Z-stacks using a Nikon Eclipse TE 2000-U microscope. Images comprising each Z-stack (1024 × 1024 pixels) were acquired (60×) over the entire dendrite tree at 0.5-μm increments. To cover the entire neuron (ending and branches), two different overlapping Z-stacks were acquired and stitched together using XuvStitch 8.1×64 (XuvTools) software. Quantification of dendritic parameters was derived from three-dimensional (3D) reconstructions of Z-stacks from deconvoluted images using the AutoQuant X3 algorithm (Media Cybernetics). Deconvoluted 3D reconstructions yielded high spatial resolution images for detailed dendritic tracing and spine classification using the IMARIS software suite (Bitplane Inc.) as previously described (14).

Neuron reconstruction and spine parameters

Details regarding the reconstruction of neurons and the morphologic classification of spines have been described (14). Briefly, an algorithm for tracing dendritic filaments was used to reconstruct the entire dendritic tree spanning a series of Z-stacks (960 × 320 μm^2). Dendritic tracing originates from the soma (diameters, 75 to 100 μm) and terminates once dendrite diameters reach 0.6 μm. Reconstructed dendritic trees are then reanalyzed for dendritic spines that can be labeled, manually verified, morphologically categorized, and quantified (15). For spines to be included in our analyses, the maximum spine length and the minimum spine end diameter were set at 2.5 and 0.4 μm, respectively. Parameters were further validated from an independent series of pilot reconstructions in both manual and semiautomatic modes. Images were compared for accuracy and consistency to ensure that selected parameters represented actual variations in dendritic structure (15).

Immunohistochemistry of synaptic proteins

Coronal sections (30 μm thick) were immunostained for the quantification of PSD-95 as described previously (14). Briefly, serial 30-μm-thick sections (five per animal) from the prelimbic area (bregma, 2.80 to 1.50 mm) were selected, and three different fields (220 × 220 μm) in each section were imaged from layers II/III of the prelimbic cortex. Sections from the mPFC sections were washed in phosphate-buffered saline (PBS) (pH 7.4), blocked for 30 min in 4% (w/v) bovine serum albumin (BSA) and 0.1% Triton X-100 (TTX), and then incubated for 24 hours in a primary antibody mixture containing 1% BSA, 0.1% TTX, and mouse anti–PSD-95 (Thermo Scientific; 1:1000). Sections were then treated for 1 hour with a mixture of goat anti-mouse immunoglobulin G tagged with Alexa Fluor 594 (1:1000), rinsed thoroughly in PBS, and sealed in an antifade mounting medium (Life Technologies).

To optimize the quantification of immunoreactive PSD-95 puncta, confocal Z-stacks were first deconvoluted using AutoQuant X3 (Media Cybernetics) software to correct z-axis distortion. High-resolution images were then exported into IMARIS (Bitplane Inc.) for 3D deconvolution using a predefined diameter threshold (0.5 μm). The density of PSD-95 was then quantified by conversion to a 3D surface, derived from confocal Z-stacks taken in 0.5-μm steps at 60×. The "surface quality threshold" and "minimum surface diameter" parameters were manually adjusted to optimize puncta detection and kept constant thereafter for all subsequent analyses.

Parihar *et al. Sci. Adv.* 2015;1:e1400256   1 May 2015

5 of 6

RESEARCH ARTICLE

Statistical analysis

Data are expressed as means ± SEM of 5 to 10 independent measurements. The level of significance was assessed by one-way ANOVA along with Bonferroni's multiple comparison using Prism data analysis software (v6.0). Correlation of spine density or PSD-95 puncta to individual DIs was performed using the Spearman rank test. Statistical significance was assigned at $P < 0.05$.

SUPPLEMENTARY MATERIALS

Supplementary material for this article is available at http://advances.sciencemag.org/cgi/content/full/1/4/e1400256/DC1
Supplementary Text
Fig. S1. Correlation of PSD-95 puncta and DI.

REFERENCES AND NOTES

1. F. A. Cucinotta, H. Nikjoo, D. T. Goodhead, The effects of delta rays on the number of particle-track traversals per cell in laboratory and space exposures. *Radiat. Res.* **150**, 115–119 (1998).
2. C. Zeitlin, D. M. Hassler, F. A. Cucinotta, B. Ehresmann, RF Wimmer-Schweingruber, DE Brinza, S. Kang, G. Weigle, S. Böttcher, E. Böhm, S. Burmeister, J. Guo, J. Köhler, C. Martin, A. Posner, S. Rafkin, G. Reitz, Measurements of energetic particle radiation in transit to Mars on the Mars Science Laboratory. *Science* **340**, 1080–1084 (2013).
3. F. Cucinotta, M. Alp, F. Sulzman, M. Wang, Space radiation risks to the central nervous system. *Life Sci. Space Res.* **2**, 54–69 (2014).
4. I. Plante, A. Ponomarev, F. A. Cucinotta, 3D visualisation of the stochastic patterns of the radial dose in nano-volumes by a Monte Carlo simulation of HZE ion track structure. *Radiat. Prot. Dosimetry* **143**, 156–161 (2011).
5. *NCRP Report No. 153* (National Council on Radiation Protection and Measurements, Bethesda, MD, 2006).
6. M. Durante, F. A. Cucinotta, Heavy ion carcinogenesis and human space exploration. *Nat. Rev. Cancer* **8**, 465–472 (2008).
7. R. A. Britten, L. K. Davis, A. M. Johnson, S. Keeney, A. Siegel, L. D. Sanford, S. J. Singletary, G. Lonart, Low (20 cGy) doses of 1 GeV/u ^{56}Fe-particle radiation lead to a persistent reduction in the spatial learning ability of rats. *Radiat. Res.* **177**, 146–151 (2012).
8. G. Lonart, B. Parris, A. M. Johnson, S. Miles, L. D. Sanford, S. J. Singletary, R. A. Britten, Executive function in rats is impaired by low (20 cGy) doses of 1 GeV/u ^{56}Fe particles. *Radiat. Res.* **178**, 289–294 (2012).
9. B. P. Tseng, E. Giedzinski, A. Izadi, T. Suarez, M. L. Lan, K. K. Tran, M. M. Acharya, G. A. Nelson, J. Raber, V. K. Parihar, C. L. Limoli, Functional consequences of radiation-induced oxidative stress in cultured neural stem cells and the brain exposed to charged particle irradiation. *Antioxid. Redox Signal.* **20**, 1410–1422 (2013).
10. R. A. Britten, L. K. Davis, J. S. Jewell, V. D. Miller, M. M. Hadley, L. D. Sanford, M. Machida, G. Lonart, Exposure to mission relevant doses of 1 GeV/nucleon ^{56}Fe particles leads to impairment of attentional set-shifting performance in socially mature rats. *Radiat. Res.* **182**, 292–298 (2014).
11. C. A. Meyers, Neurocognitive dysfunction in cancer patients. *Oncology* **14**, 75–79; discussion 79, 81–72, 85 (2000).
12. J. M. Butler, S. R. Rapp, E. G. Shaw, Managing the cognitive effects of brain tumor radiation therapy. *Curr. Treat. Options Oncol.* **7**, 517–523 (2006).
13. V. K. Parihar, B. D. Allen, K. K. Tran, N. N. Chmielewski, B. M. Craver, V. Martirosian, J. M. Morganti, S. Rosi, R. Vlkolinsky, M. M. Acharya, G. A. Nelson, A. R. Allen, C. L. Limoli, Targeted overexpression of mitochondrial catalase prevents radiation-induced cognitive dysfunction. *Antioxid. Redox Signal.* **22**, 78–91 (2015).
14. V. K. Parihar, C. L. Limoli, Cranial irradiation compromises neuronal architecture in the hippocampus. *Proc. Natl. Acad. Sci. U.S.A.* **110**, 12822–12827 (2013).
15. V. K. Parihar, J. Pasha, K. K. Tran, B. M. Craver, M. M. Acharya, C. L. Limoli, Persistent changes in neuronal structure and synaptic plasticity caused by proton irradiation. *Brain Struct. Funct.* **220**, 1161–1171 (2015).
16. J. D. Bremner, J. H. Krystal, S. M. Southwick, D. S. Charney, Functional neuroanatomical correlates of the effects of stress on memory. *J. Trauma. Stress* **8**, 527–553 (1995).
17. W. E. Kaufmann, H. W. Moser, Dendritic anomalies in disorders associated with mental retardation. *Cereb. Cortex* **10**, 981–991 (2000).
18. M. Nishimura, X. Gu, J. W. Swann, Seizures in early life suppress hippocampal dendrite growth while impairing spatial learning. *Neurobiol. Dis.* **44**, 205–214 (2011).
19. D. J. Selkoe, Alzheimer's disease is a synaptic failure. *Science* **298**, 789–791 (2002).
20. S. Takashima, K. Iida, T. Mito, M. Arima, Dendritic and histochemical development and ageing in patients with Down's syndrome. *J. Intellect. Disabil. Res.* **38** (Pt. 3), 265–273 (1994).
21. M. van Spronsen, C. C. Hoogenraad, Synapse pathology in psychiatric and neurologic disease. *Curr. Neurol. Neurosci. Rep.* **10**, 207–214 (2010).
22. G. R. Barker, F. Bird, V. Alexander, E. C. Warburton, Recognition memory for objects, place, and temporal order: A disconnection analysis of the role of the medial prefrontal cortex and perirhinal cortex. *J. Neurosci.* **27**, 2948–2957 (2007).
23. G. R. Barker, E. C. Warburton, When is the hippocampus involved in recognition memory? *J. Neurosci.* **31**, 10721–10731 (2011).
24. J. J. Radley, C. M. Arias, P. E. Sawchenko, Regional differentiation of the medial prefrontal cortex in regulating adaptive responses to acute emotional stress. *J. Neurosci.* **26**, 12967–12976 (2006).
25. F. Sotres-Bayon, D. Sierra-Mercado, E. Pardilla-Delgado, G. J. Quirk, Gating of fear in prelimbic cortex by hippocampal and amygdala inputs. *Neuron* **76**, 804–812 (2012).
26. C. Varela, S. Kumar, J. Y. Yang, M. A. Wilson, Anatomical substrates for direct interactions between hippocampus, medial prefrontal cortex, and the thalamic nucleus reuniens. *Brain Struct. Funct.* **219**, 911–929 (2014).
27. E. I. Charych, B. F. Akum, J. S. Goldberg, R. J. Jörnsten, C. Rongo, J. Q. Zheng, B. L. Firestein, Activity-independent regulation of dendrite patterning by postsynaptic density protein PSD-95. *J. Neurosci.* **26**, 10164–10176 (2006).
28. G. F. Woods, W. C. Oh, L. C. Boudewyn, S. K. Mikula, K. Zito, Loss of PSD-95 enrichment is not a prerequisite for spine retraction. *J. Neurosci.* **31**, 12129–12138 (2011).
29. Y. Yoshihara, M. De Roo, D. Muller, Dendritic spine formation and stabilization. *Curr. Opin. Neurobiol.* **19**, 146–153 (2009).
30. J. Bourne, K. M. Harris, Do thin spines learn to be mushroom spines that remember? *Curr. Opin. Neurobiol.* **17**, 381–386 (2007).
31. D. Keith, A. El-Husseini, Excitation control: Balancing PSD-95 function at the synapse. *Front. Mol. Neurosci.* **1**, 4 (2008).
32. D. Preissmann, G. Leuba, C. Savary, A. Vernay, R. Kraftsik, I. M. Riederer, F. Schenk, B. M. Riederer, A. Savioz, Increased postsynaptic density protein-95 expression in the frontal cortex of aged cognitively impaired rats. *Exp. Biol. Med.* **237**, 1331–1340 (2012).
33. D. M. Yilmazer-Hanke, Morphological correlates of emotional and cognitive behaviour: Insights from studies on inbred and outbred rodent strains and their crosses. *Behav. Pharmacol.* **19**, 403–434 (2008).